scientific reports

OPEN

Relationship between renal oxidative stress levels and disease severity in patients with chronic kidney disease assessed by [Cu-64] ATSM PET/MRI

Ya'nan Huang[1,2], Yudai Nishikawa[3], Tetsuya Mori[1], Munenobu Nogami[1], Akira Makino[1], Yasushi Kiyono[1], Tadashi Toyama[3] & Hidehiko Okazawa[1✉]

The purpose of the study was to investigate renal oxidative stress (OS) and its relationship with disease severity in patients with chronic kidney disease (CKD) using positron emission tomography coupled with magnetic resonance imaging (PET/MRI), employing ^{64}Cu-diacetyl-bis(N^4-methylthiosemicarbazonate) (^{64}Cu-ATSM) as the PET tracer for OS imaging. Thirty patients with CKD (66.4 ± 8.2 y.o.) and seven healthy controls (HC) subjects (58.3 ± 3.8 y.o.) underwent ^{64}Cu-ATSM PET/MRI. Participants were categorized into three groups based on their estimated glomerular filtration rate (eGFR): HC, mild CKD (stages 2-3a), and advanced CKD (stages 3b-5). All subjects underwent 30-min dynamic PET/MRI starting with the injection of ^{64}Cu-ATSM to evaluate renal blood flow (RBF) and OS levels. RBF (mL/min/100 g) images were calculated from the first 3 min PET data, and standardized uptake value (SUV) images were obtained from delayed frames of 15–30 min after injection. The ^{64}Cu-ATSM SUV images were corrected to RBF-adjusted SUV using individual RBF images to estimate the OS levels of individual kidneys using the following equation: adjusted OS index (aOSi) = (SUV/RBF) x100. Significant correlation was observed between eGFR and RBF ($r = 0.81$, $P < 0.001$). RBF in patients with advanced CKD is significantly lower than that in HC ($P < 0.001$) and patients with mild CKD ($P = 0.004$). ^{64}Cu-ATSM SUV did not differ significantly among the three groups ($P = 0.171$). ^{64}Cu-ATSM SUVs did not correlate with creatinine in the HC subjects or in the patients with CKD. However, these values did correlate with eGFR ($r = 0.33$, $P = 0.049$) in all subjects, whereas the CKD patients showed no significant correlation. Following RBF correction, the aOSi demonstrated significant correlations with creatinine ($r = 0.75$, $P < 0.001$), eGFR ($r = -0.65$, $P < 0.001$), and CKD stages ($r = 0.57$, $P < 0.001$) in all subjects. This preliminary study has revealed that ^{64}Cu-ATSM PET may provide a estimate of renal OS reasonably in CKD patients noninvasively. Increased aOSi values were correlated with the CKD stages and creatinine levels, suggesting that OS increases with the severity of renal dysfunction.

Chronic kidney disease (CKD) is defined as an abnormality in kidney structure or function that has existed for a minimum of three months. CKD is an important public health issue worldwide, with significant health implications. Information on the prevalence of CKD is available for 73.9% of countries, with a median global prevalence of 9.5%[1]. Microvascular blood flow in the kidney is an important indicator of pathophysiology, because abnormal perfusion could be either a cause or a consequence of disease development[2]. Therefore, the evaluation of renal blood flow (RBF) is important for understanding the pathophysiology of CKD. RBF can be estimated using blood data and substances such as para-aminohippuric acid and inulin, or by endogenous markers such as creatinine and cystatin C[3]. These methods use blood data to evaluate the average RBF of the bilateral kidneys, whereas imaging techniques such as dynamic renal scintigraphy, MRI-ASL, DCE-MRI, and PET-RBF have been developed to assess the RBF of individual kidneys[2–6]. Our previous study revealed a correlation between RBF

[1]Biomedical Imaging Research Center, University of Fukui, 23-3, Matsuoka-Shimaizuki, Eiheiji-cho, Fukui 910-1193, Japan. [2]Department of Radiology, Shaoxing People's Hospital, Shaoxing, China. [3]Department of Nephrology, Faculty of Medical Sciences, University of Fukui, Fukui, Japan. ✉email: okazawa@u-fukui.ac.jp

and renal function[3]. Conventional renal scintigraphy can also evaluate glomerular filtration rate (GFR), another important indicator of renal function.

Oxidative stress (OS), a crucial factor in CKD, is caused by an imbalance between pro-oxidants and antioxidants, typically due to the excessive generation of reactive oxygen species (ROS), which induce damages to cellular proteins, lipids, and DNA, and also increase inflammation[7]. There is growing evidence that ROS causes OS, inflammation and fibrosis, which in turn contribute to redox imbalance and renal dysfunction[7–9]. The underlying pathophysiological mechanisms contributing to this process include activation of the renin-angiotensin-aldosterone system (RAAS), reduction in the GFR, elevated blood pressure, and inflammatory responses[8]. In addition, OS is linked to the development of several CKD complications, including cardiovascular disease and inflammation[7,8,10,11]. Given the critical role of OS in CKD progression and its associated complications, renal OS assessment, in addition to quantitative RBF measurement, is important to gain a comprehensive understanding of the underlying pathophysiology of CKD. Advanced oxidative protein products (AOPPs) and 8-isoprostanes are systemic markers that indirectly reflect renal OS status[12,13], whereas PET imaging would effectively delineate changes in individual renal OS and provide potential applications for personalized medicine such as selection of therapeutic options including antioxidant therapy and their monitoring.

Cu (II)-diacetyl-bis(N^4-methylthiosemicarbazonate) (Cu-ATSM) with radioactive copper is a positron emission tomography (PET) tracer designed for detecting hypoxia and imaging OS in the brain, heart, and tumors[14–20]. The cited studies have shown that early-phase images obtained after tracer injection reveal blood flow, whereas later-phase images (10–15 min post-injection or later) reveal Cu-ATSM retention[16,17]. We developed a method for RBF measurement using dynamic ^{64}Cu-ATSM PET data and demonstrated its reliability by comparing PET-RBF values with the estimated RBF (eRBF) calculated from the estimated GFR (eGFR) as well as the RBF obtained from arterial spin labeling MRI (MRI-ASL)[3]. In the study, ^{64}Cu-ATSM standardized uptake values (SUVs) obtained from later-phase images, which were expected to reflect the OS levels of the kidneys, did not show differences between healthy control (HC) subjects and patients with CKD. This is probably occurred because the total amount of ^{64}Cu-ATSM reaching the kidneys differed between CKD patients and HC subjects as a result of RBF reduction in the CKD patients. SUV values reflect only the retention of tracer that reaches the tissues, and decrease in blood flow in the organ affects the total retention. Therefore, ^{64}Cu-ATSM SUVs should be corrected for individual RBF to assess the renal OS correctly.

The purpose of the ^{64}Cu-ATSM PET/MRI study presented here was to evaluate renal OS levels, and analyze the relationship between renal OS and disease severity in patients with CKD, thus, the role of OS in the pathophysiology and progression of CKD could be clarified. To this end, we measured RBF from early-phase images and applied them to correct SUV images and to estimate OS levels in the kidney appropriately.

Materials and methods
Subjects
Thirty patients (nine females) with CKD and seven HC subjects (two females) participated in this study. Of the 30 patients, 12 had diabetic kidney disease (DKD), eight had nephrosclerosis (NS), three had IgA glomerulonephritis (IgAGN), three had non-IgA glomerulonephritis (non-IgAGN), two had minimal change nephrotic syndrome (MCNS), and two had drug-induced nephropathy. IgA/non-IgAGN and MCNS were determined by biopsy. Serum creatinine levels were measured by the Division of Clinical Laboratories at the University of Fukui Hospital (Fukui, Japan) within a week before ^{64}Cu-ATSM PET/MRI, using the enzyme colorimetry method. The eGFR was calculated from the serum creatinine (cr) level using the following equation[21]:

$$\mathrm{eGFRcr}\left(\mathrm{mL/min/1.73m^2}\right) \;=\; 194 \,\times\, \mathrm{serum\ cr}^{-1.094} \times\, \mathrm{age}^{-0.287}\,(\times\,0.739\ \mathrm{for\ females}).$$

CKD was categorized into two groups: mild CKD (stages 2–3a) and advanced CKD (stages 3b–5), based on the eGFR categories corresponding with the current CKD nomenclature specified by Kidney Disease: Improving Global Outcomes (KDIGO)[1]. This study was approved by the Research Ethics Committee of the University of Fukui Hospital (approval number: 20170053). The study was conducted in accordance with the principles of the Declaration of Helsinki. All participants provided written informed consent before undergoing the PET/MRI scans.

Dynamic ^{64}Cu-ATSM PET/MRI imaging
^{64}Cu was produced using an RDS Eclipse biomedical cyclotron (Siemens, Göteborg, Sweden). The details were described elsewhere[22,23]. In brief, a gold disc (25 mm in diameter, 2 mm thick) with a central dimple filled with enriched ^{64}Ni (> 99%) was bombarded with 11 MeV protons. ^{64}Cu was separated using the established procedure, and ^{64}Cu-ATSM was produced by stirring ^{64}Cu-saline and ATSM in DMSO[22].

All participants underwent ^{64}Cu-ATSM PET/MRI using a whole-body scanner (Signa PET/MR ver. 26, GE Healthcare, Milwaukee, WI, USA). This scanner enables the simultaneous acquisition of PET data across 89 image slices (slice thickness: 2.78 mm) in three dimensions (3D). Performance tests indicated that the transaxial intrinsic resolution of the PET images ranged between 4.2 mm and 4.3 mm full width at half maximum (FWHM). According to the manufacturer's instructions, the PET/MRI scanner was calibrated before ^{64}Cu-ATSM PET/MRI was performed, using a dose calibrator (CRC-12, Capintec Inc., Florham Park, NJ, USA) and a pool phantom with ^{18}F solution.

A 30-minute list-mode 3D PET scan was initiated using the time-of-flight acquisition mode at the time of bolus injection of ^{64}Cu-ATSM (250–430 MBq) into the antecubital vein. Multiple MRI sequences were acquired during the PET scan, including T1- and T2-weighted images (WI), as well as LAVA-FLEX (GE Healthcare) for PET attenuation correction (AC). Dynamic PET data were reconstructed using the 3D-ordered subset expectation maximization (OSEM) method and the point spread function modeling algorithm in 34 frames

(12×5s, 6×10s, 3×20s, 4×30s, 5×60s, and 4×5 min). The following OSEM parameters were utilized for the reconstruction of PET images: subsets, 16; iterations, 2; trans-axial post-Gaussian filter cutoff, 4 mm in a 384 mm field of view; pixel size, 3×3 mm^2. ^{64}Cu-ATSM uptake in the kidney was assessed using a SUV image converted from static PET data 15–30 min post-injection. The SUV calculation was conducted as follows; SUV = (tissue radioactivity concentration)/ [(injection dose)/ (body weight)].

Calculation of RBF and adjusted OS index

The RBF image (mL/min/100 g) was calculated from the first 3-min frames of the dynamic PET data with a one-tissue compartment model. The details of the RBF calculation from the dynamic PET data has been described elsewhere[3,24]. Circular regions of interest (ROIs; diameter, 10 mm) were drawn in the abdominal aorta at the level of the renal artery using three image slices of early phase PET images to estimate the arterial input function. The mean ROI values of the three slices were calculated for each frame as the arterial radioactivity at the mid-frame time of the dynamic PET data.

Ten circular ROIs, 10 mm in diameter, were placed on each kidney using 3–6 slices (three slices were used for most subjects, and four to six slices were used in cases with severe renal atrophy) on LAVA-FLEX MRI images acquired during dynamic PET to obtain the cortical RBF and SUV (Fig. 1). To evaluate the renal tissue OS quantitatively, the RBF-adjusted SUV was calculated from the SUV with a correction for RBF. In this new parameter, SUV is corrected to avoid the influence of RBF on tracer accumulation, which would delineate the relative OS level in the tissue[14,17,19], and we define it as adjusted OS index (aOSi), i.e., aOSi = [SUV/ RBF (mL/min/100 g)] x 100 (g), where the regional RBF was corrected into the unit of (mL/min/g). aOSi images were also calculated using the same equation.

Statistical analysis

Numerical data are presented in the form of the mean ± standard deviation (SD). Before comparisons were drawn, normal distribution and variance homogeneity tests were performed on the parameters for each group. If the data conformed to a normal distribution and had equal variances, the overall differences among the three groups were compared using an analysis of variance (ANOVA). Tukey's Honestly Significant Difference (HSD) test was used as a post-hoc test. If the data were not normally distributed or the variances were unequal, the overall differences among the three groups were compared using the Kruskal-Wallis test, and Dunn's test was used as a post-hoc test. The Pearson correlation was used to analyze the relationships between the parameters. The relationship between CKD stages and the aOSi was analyzed using the Spearman correlation. All statistical analyses were performed using R (version 4.4.0; https://www.r-project.org/). Values with $P < 0.05$ were considered statistically significant. P-values were adjusted using the Benjamini-Hochberg method.

Results

There were nine patients in the mild CKD group (five in stage 2 and four in stage 3a) and 21 patients in the advanced CKD group (nine in stage 3b, eight in stage 4, and four in stage 5). The demographics and mean values for each group are listed in Table 1. The age, creatinine level, and eGFR of patients with advanced CKD were significantly higher than those of subjects in the HC group. Creatinine levels and eGFR of patients with advanced CKD were significantly higher than those of patients with mild CKD.
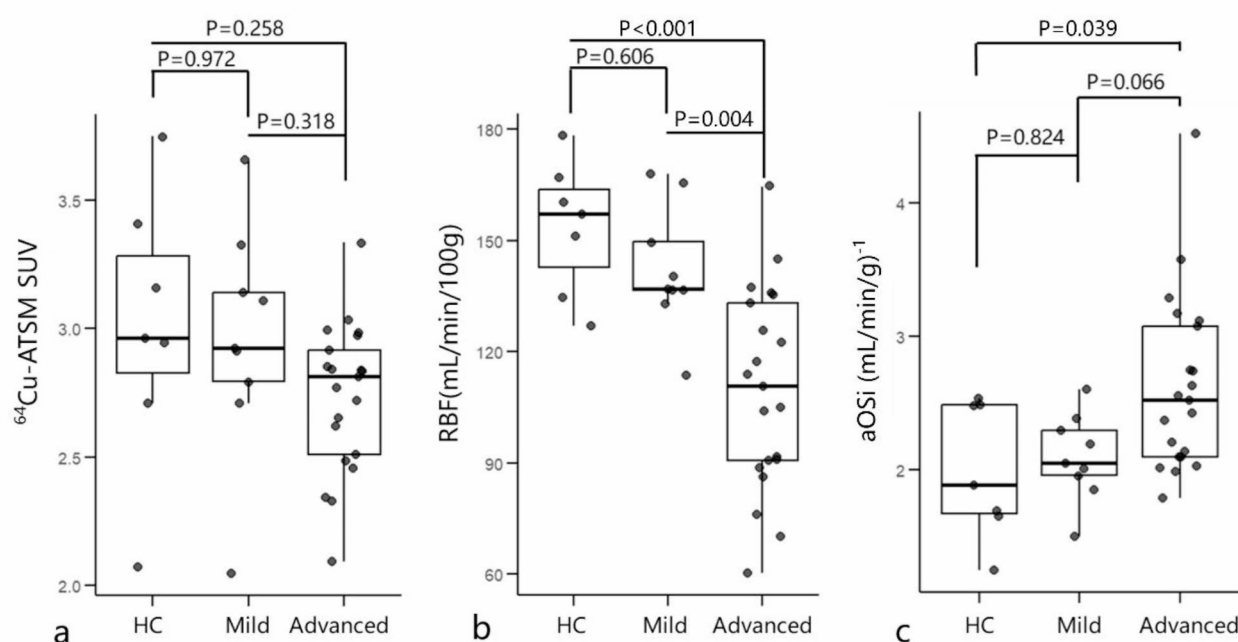
The SUVs did not differ significantly among the three groups (Table 1; Fig. 2a). The RBF in patients with advanced CKD was significantly lower than that in the HC group (Fig. 2b, $P < 0.001$) and in patients with mild CKD (Fig. 2b, $P = 0.004$). The aOSi for patients with advanced CKD was significantly higher than that for the HC
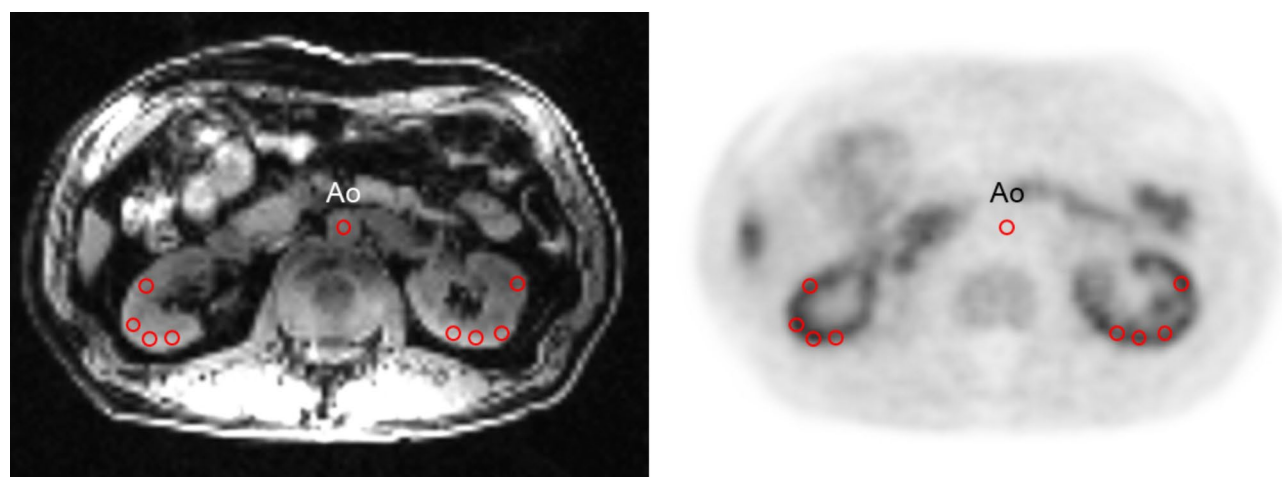
Fig. 1. Example of ROIs set at the same slice level on LAVA-FLEX MRI (left) and PET (right) images. The locations of ROIs are exactly the same because the two images were acquired simultaneously. Ao indicates abdominal aorta.

	HC	Mild CKD	Advanced CKD
Subjects (Male : Female)	7 (5:2)	9 (6:3)	21 (15:6)
Age	58.3 ± 3.8	65.1 ± 9.3	67.0 ± 7.9†
Creatinine (mg/dL)	0.77 ± 0.08	0.96 ± 0.20*	2.53 ± 1.99†*
eGFR (mL/min/1.73m²)	71.4 ± 5.2	60.1 ± 9.8*	26.7 ± 12.0†*
^{64}Cu-ATSM dose (MBq)	348.4 ± 45.8	356.1 ± 33.4	373.2 ± 37.1
RBF (mL/min/100 g)	153.6 ± 17.9	142.2 ± 16.8*	109.8 ± 27.1†*
SUV	3.0 ± 0.5	2.9 ± 0.5	2.7 ± 0.3
aOSi (mL/min/g)⁻¹	2.0 ± 0.5	2.1 ± 0.3	2.6 ± 0.7†

Table 1. Participants' demographics and values of biomarkers (mean ± SD). †$P < 0.05$ compared with healthy control (HC) group. *$P < 0.05$ compared between mild and advanced chronic kidney disease (CKD) groups. The Kruskal-Walli's test was used for creatinine and aOSi comparisons. Mild CKD patients are in stage G2-G3a and advanced CKD patients are in stage G3b-G5.


Fig. 2. Box and whisker plots of ^{64}Cu-ATSM SUV, RBF, and aOSi of the three designated groups. SUVs do not differ significantly among the groups (**a**), and RBF in patients with advanced CKD is significantly lower than those in other groups (**b**). The aOSi for patients with advanced CKD is significantly higher than that for the HC group (Kruskal-Walli's test), but not significantly different from that for patients with mild CKD (**c**).

group (Fig. 2c, $P = 0.039$). The aOSi for patients with mild CKD was similar to that for subjects in the HC group and tended to be lower than that for patients with advanced CKD (Fig. 2c, $P = 0.066$).

Figure 3 shows good correlations between RBF and eGFR (Fig. 3a, $r = 0.81$, $P < 0.001$) and between RBF and creatinine (Fig. 3b, $r = -0.66$, $P < 0.001$) in all subjects, indicating that the renal dysfunction was associated with decreased RBF. The relationship between the ^{64}Cu-ATSM SUV and other biomarkers is illustrated in Fig. 4. The ^{64}Cu-ATSM SUV was not correlated with creatinine across all participants (Fig. 4a), yet demonstrated slight correlations with eGFR (Fig. 4b, $r = 0.33$, $P = 0.049$) and CKD stages (Fig. 4c, $r = -0.34$, $P = 0.040$). In patients with CKD, no correlation was observed between the ^{64}Cu-ATSM SUV and other biomarkers (Fig. 4d–f). When comparing the aOSi and other biomarkers, significant correlations were found with creatinine and eGFR, in all participants ($r = 0.75$ and -0.65, respectively) as well as in CKD patients only ($r = 0.78$ and -0.64, respectively) (Fig. 5). The aOSi was also correlated with the CKD stages, with ($r = 0.57$) or without the HC group ($r = 0.58$) (Fig. 5c and f).

Figure 6 shows representative images for a HC subject and patients with mild and advanced CKD, with respect to ^{64}Cu-ATSM PET images of the SUV, RBF and aOSi. The advanced CKD patient (right column) had
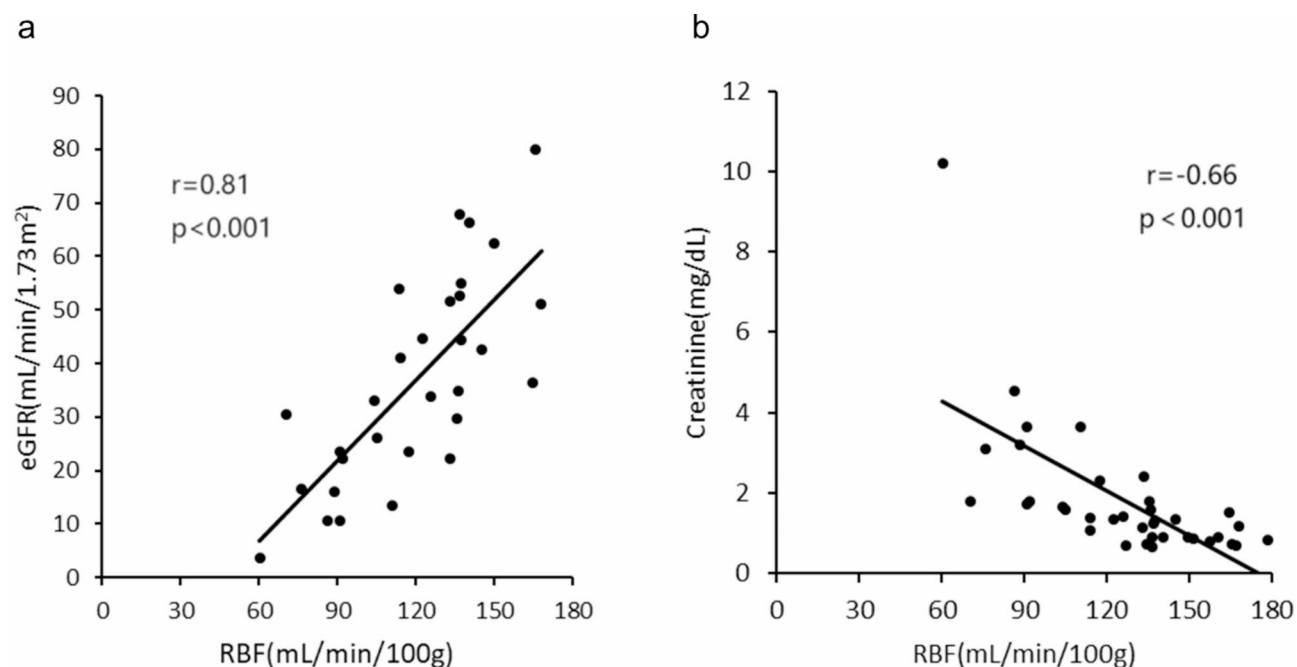
Fig. 3. Relationship between eGFR, creatinine and RBF. Scatter plots of RBF vs. eGFR (**a**) and RBF vs. creatinine (**b**) show significant correlations ($r = 0.81$ and $r = -0.66$, respectively).
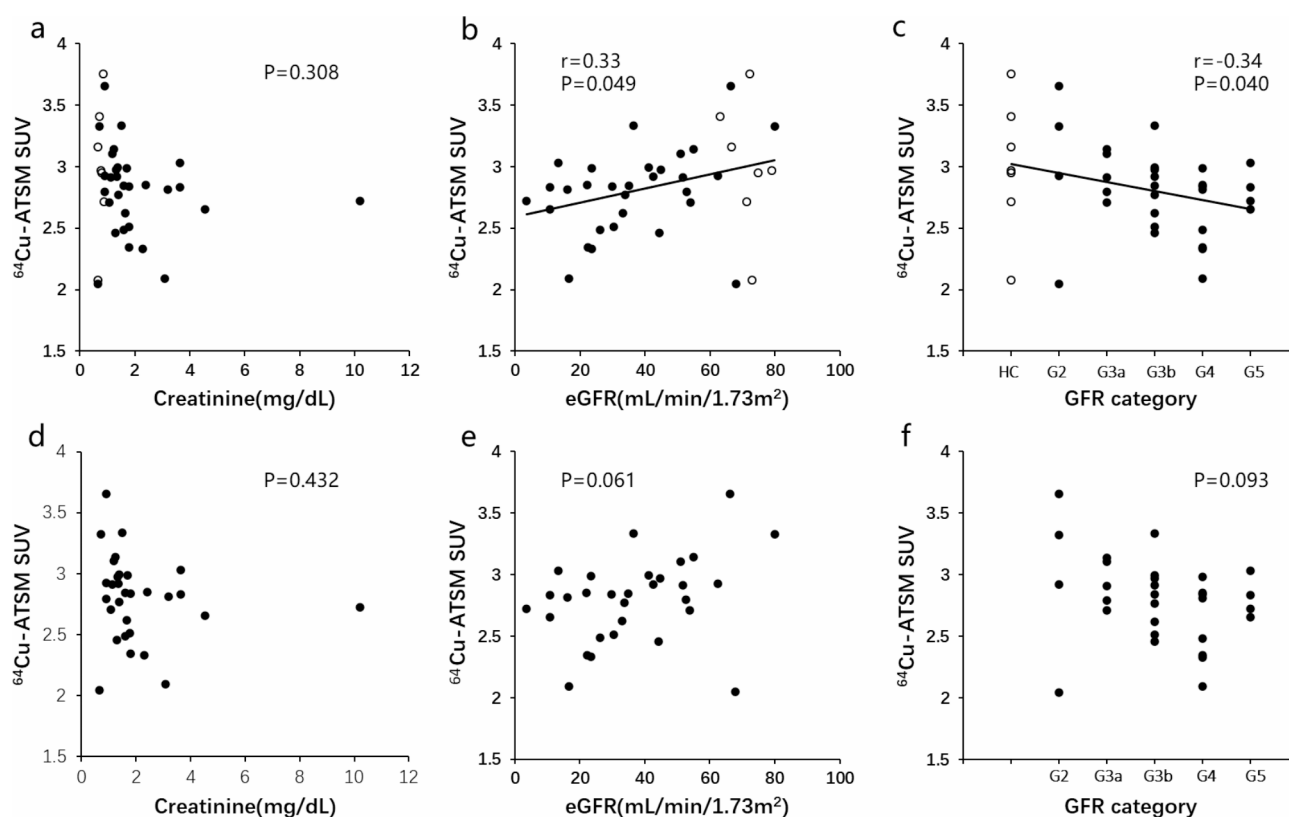

Fig. 4. Scatter plots of the ^{64}Cu-ATSM SUV vs. other biomarkers. In all subjects (top row), the SUV was not correlated with creatinine ((**a**), $P = 0.308$); however, it demonstrated slight correlations with eGFR ((**b**), $r = 0.33$, $P = 0.049$) and CKD stages ((**c**), $r = -0.34$, $P = 0.040$). Circles (o) represent healthy control subjects and filled circles (●) represent patients with CKD. In the CKD patients (bottom row), the SUV was not correlated with creatinine ((**d**), $P = 0.432$), eGFR ((**e**), $P = 0.061$), or CKD stages ((**f**), $P = 0.093$).
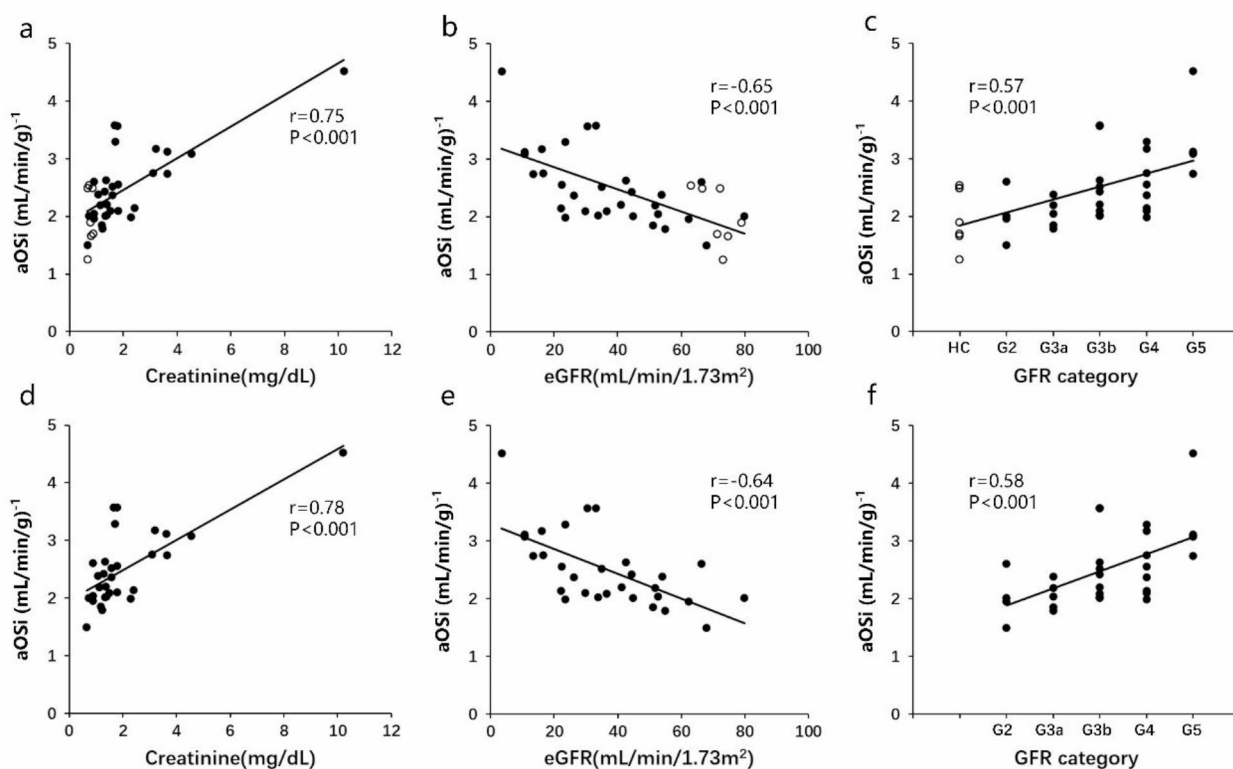
Fig. 5. Scatter plots of the aOSi vs. other biomarkers. In all participants (top row) and in CKD patients (bottom row), the aOSi was positively correlated with creatinine ((**a,d**), $r = 0.75, 0.78$; $P < 0.001$) and CKD category ((**c,f**), $r = 0.57, 0.58$; $P < 0.001$), and inversely correlated with eGFR ((**b,e**), $r = -0.65, -0.64$; $P < 0.001$). Circles (o) represent healthy control subjects and filled circles (●) represent patients with CKD.
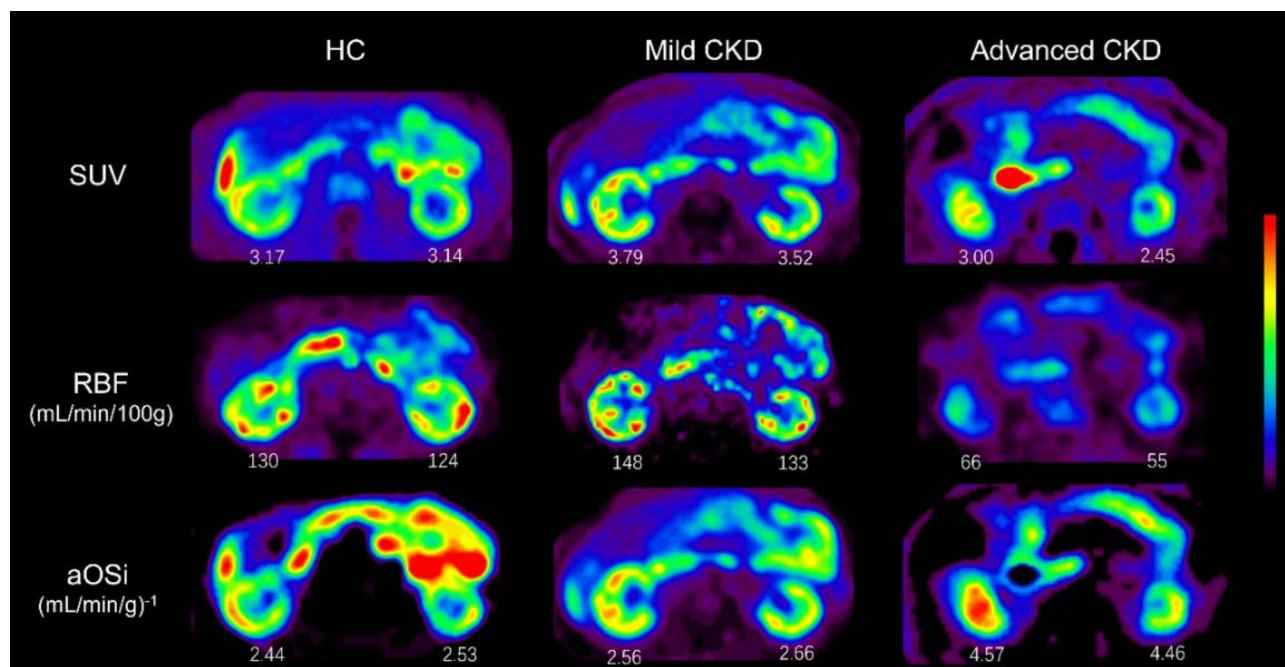
Fig. 6. Representative ^{64}Cu-ATSM PET images of SUV, RBF, and aOSi for a healthy control (HC), patients with mild and advanced chronic kidney disease (CKD). The number below each kidney represents the mean values of the corresponding parameter.

atrophic kidneys, decreased RBF and increased aOSi compared to those images of the HC subject and the patient with mild CKD.

Discussion

In the present study, the renal aOSi was significantly correlated with creatinine level, eGFR, and the CKD stage, for CKD patients as well as for all participants. The eGFR also correlated well with the RBF, which is consistent with the results of our previous study[3]. The ^{64}Cu-ATSM SUV was not correlated with creatinine and slightly correlated with eGFR ($r = 0.33$) and CKD stage ($r = -0.34$) when including all subjects; however, no significant correlation was observed for the CKD patients. These findings indicate that renal OS level assessed by aOSi is associated with the CKD stage and ^{64}Cu-ATSM PET imaging is a promising method for evaluating renal OS non-invasively.

Cu-ATSM labeled with various Cu isotopes (^{60}Cu, ^{61}Cu, ^{62}Cu, or ^{64}Cu) has been developed as PET tracers for imaging hypoxic tissues and regions of OS[15,20]. Hypoxic tissue increases ROS production, inducing additional oxidative stress and damage to organs. The mechanism of ^{64}Cu-ATSM accumulation is based on the reduction of divalent copper [Cu(II)] in the compound to monovalent copper [Cu(I)] under over-reduced conditions, where Cu(I) is eventually irreversibly trapped in cells[14]. Recent studies reported that patients with neurodegenerative diseases demonstrated greater Cu-ATSM SUV in brain regions responsible for early Alzheimer's disease (eAD), amyotrophic lateral sclerosis (ALS), and Parkinson's disease[17,19,25]. Several other studies also demonstrated that OS in the brain, heart, and tumors can be evaluated using Cu-ATSM PET imaging, the results of which correlate well with disease progression[14–20].

In the present study, ^{64}Cu-ATSM SUVs from later-phase images did not differ significantly between patients with CKD and HC subjects, notwithstanding the reduction of RBF in patients' kidneys, suggesting that the ^{64}Cu-ATSM SUV may not sufficiently reflect the OS levels in the kidney. Since the RBF in patients with advanced CKD was significantly lower than that in HC subjects and patients with mild CKD, the amount of ^{64}Cu-ATSM reaching the kidney tissue was considered to be limited. To assess renal OS using ^{64}Cu-ATSM PET accurately, SUV values should be corrected for RBF reduction to avoid the influence of different amounts of tracer arrival. As mentioned in the previous study on eAD, it is important to consider the regional differences in blood flow when making quantitative comparisons of OS levels[25].

Following RBF correction, patients with advanced CKD demonstrated a significantly higher aOSi compared to HC subjects, although patients with mild CKD did not show a significant difference. A previous study indicated that plasma 8-isoprostanes, a marker of oxidative stress, was elevated in patients with stage 3–5 CKD, compared to patients with early CKD and HC subjects, whereas early CKD patients and control subjects showed no differences[12]. Similarly, Villalpando-Sánchez DC, et al. reported that AOPPs were significantly more prevalent in stage 4–5 CKD compared to early CKD[13]. These results are consistent with our results, although the difference in the aOSi between mild CKD and advanced CKD was not found to be significant in this study ($P = 0.066$). In the early stages of CKD, the kidneys may compensate for the impaired function by increasing the workload of the remaining nephrons. This adaptive change may temporarily mask overt signs of symptoms in the early stages of CKD.

In the present study, the aOSi were significantly correlated with creatinine levels, eGFR, and GFR categories in all participants as well as patients with CKD. Previous studies have reported that the AOPPs were positively correlated with creatinine levels, and that there were significant inverse correlations between plasma 8-isoprostanes, AOPPs, and eGFR in patients with CKD[13,26]. Hypoxia in the kidneys may induce swelling of the proximal tubular cells, increase intrarenal resistance (IRR = arterial pressure/RBF) and reduce blood flow throughout the renal cortex, which may accelerate GFR decline and CKD dysfunction[7,27]. AOPPs and 8-isoprostanes are systemic markers that indirectly reflect renal OS status, whereas ^{64}Cu-ATSM PET delineates individual renal OS changes effectively as PET images. This capability suggests promising applications in personalized medicine, allowing for more targeted treatment strategies and improved management of kidney-related diseases.

Antioxidants therapy may be a potential treatment option for patients with CKD. Several preclinical studies have indicated that antioxidants such as isoliquiritigenin and BAY-543, a soluble guanylyl cyclase activator, can enhance renal total antioxidant capacity[28,29]. In non-dialysis patients with stage 3–5 CKD, the antioxidant sulforaphane (SFN) improved the antioxidant system[30]. These results suggest that antioxidants can slow the kidney dysfunction of caused by OS in CKD. ^{64}Cu-ATSM PET for the assessment of renal OS may be a valuable tool for monitoring and optimizing antioxidant therapy in patients with CKD. If the potential role of antioxidants in reducing renal OS is identified and applied to CKD, ^{64}Cu-ATSM PET will be a promising tool to assess therapeutic efficacy.

A limitation of this study is its relatively small sample size. Further studies with larger sample sizes are needed to confirm the results of differences in OS levels across each CKD stage, as well as across subgroups, based on various clinical causes and phenotypes.

Conclusions

Increased aOSi of the kidney, RBF-adjusted SUV to estimate tissue OS level, is related to the renal function and CKD stage, especially in advanced CKD (G3b–G5). PET-OS imaging with ^{64}Cu-ATSM and RBF correction may be a promising tool to improve our understanding of CKD pathogenesis and to monitor further antioxidant therapy.

Data availability

The datasets used and/or analyzed during the current study are available from the corresponding author on reasonable request.

References

1. Bello, A. K. et al. An update on the global disparities in kidney disease burden and care across world countries and regions. *Lancet Glob Health* **12**(3), e382–e395 (2024).
2. Wu, W. C., Su, M. Y., Chang, C. C., Tseng, W. Y. & Liu, K. L. Renal perfusion 3-T MR imaging: a comparative study of arterial spin labeling and dynamic contrast-enhanced techniques. *Radiology* **261**(3), 845–853 (2011).
3. Nishikawa, Y. et al. Feasibility of renal blood Flow Measurement using 64Cu-ATSM PET/MRI: a quantitative PET and MRI study. *Diagnostics* **13**(10), 1685 (2023).
4. Alhummiany, B. A. et al. Bias and Precision in magnetic resonance imaging-based estimates of Renal Blood Flow: Assessment by Triangulation. *J. Magn. Reson. Imaging* **55**(4), 1241–1250 (2022).
5. Langaa, S. S. et al. Estimation of renal perfusion based on measurement of rubidium-82 clearance by PET/CT scanning in healthy subjects. *EJNMMI Phys.* **8**(1), 43 (2021).
6. Spiliotopoulou, M. et al. 99mTc-DTPA dynamic SPECT/CT renogram in adults: feasibility and diagnostic benefit. *Nucl. Med. Commun.* **45**(8), 673–682 (2024).
7. Daenen, K. et al. Oxidative stress in chronic kidney disease. *Pediatr. Nephrol.* **34**(6), 975–991 (2019).
8. Kishi, S., Nagasu, H., Kidokoro, K. & Kashihara, N. Oxidative stress and the role of redox signalling in chronic kidney disease. *Nat. Rev. Nephrol.* **20**(2), 101–119 (2024).
9. Webster, A. C., Nagler, E. V., Morton, R. L. & Masson, P. Chronic kidney disease. *Lancet* **389**(10075), 1238–1252 (2017).
10. Frąk, W. et al. Role of Uremic Toxins, oxidative stress, and renal fibrosis in chronic kidney disease. *Antioxidants* **13**(6), 687 (2024).
11. Srivastava, A., Tomar, B., Sharma, D. & Rath, S. K. Mitochondrial dysfunction and oxidative stress: role in chronic kidney disease. *Life Sci.* **319**, 121432 (2023).
12. Qaisar, R., Burki, A., Karim, A., Ustrana, S. & Ahmad, F. The Association of Intestinal Leak with Sarcopenia and physical disability in patients with various stages of chronic kidney disease. *Calcif Tissue Int.* **115**(2), 132–141 (2024).
13. Villalpando-Sánchez, D. C. et al. Advanced oxidative protein products had a diagnostic accuracy for identifying chronic kidney Disease in Adult Population. *Metabolites* **14**(1), 37 (2024).
14. Fujibayashi, Y. et al. Copper-62-ATSM: a new hypoxia imaging agent with high membrane permeability and low redox potential. *J. Nucl. Med.* **38**(7), 1155–1160 (1997).
15. Lewis, J. S. et al. Delineation of hypoxia in canine myocardium using PET and copper(II)-diacetyl-bis(N4-methylthiosemicarbazone). *J. Nucl. Med.* **43**(11), 1557–1569 (2002).
16. Isozaki, M. et al. Feasibility of 62Cu-ATSM PET for evaluation of brain ischaemia and misery perfusion in patients with cerebrovascular disease. *Eur. J. Nucl. Med. Mol. Imaging* **38**(6), 1075–1082 (2011).
17. Ikawa, M. et al. Increased oxidative stress is related to disease severity in the ALS motor cortex: a PET study. *Neurology* **84**(20), 2033–2039 (2015).
18. Li, F., Jørgensen, J. T., Forman, J., Hansen, A. E. & Kjaer, A. 64Cureflectsflects pO_2 Levels in Human Head and Neck Cxenograftsgraftnotut Not in Colorectal Cxenograftsgrcomparisonarison with $64CuCl_2$. *J. Nucl. Med.* **57**(3), 437–443 (2016).
19. Neishi, H. et al. Precise Evaluation of Striatal Oxidative Stress Corrected for Severity of Dopaminergic Neuronal Degeneration in patients with Parkinson's Disease: a study with 62Cu-ATSM PET and 123I-FP-CIT SPECT. *Eur. Neurol.* **78**(3–4), 161–168 (2017).
20. Xie, F. & Wei, W. [64Cu]Cu-ATSM: an emerging theranostic agent for cancer and neuroinflammation. *Eur. J. Nucl. Med. Mol. Imaging* **49**(12), 3964–3972 (2022).
21. Matsuo, S. et al. Collaborators developing the Japanese equation for estimated GFR. Revised equations for estimated GFR from serum creatinine in Japan. *Am. J. Kidney Dis.* **53**(6), 982–992 (2009).
22. Obata, A. et al. Production of therapeutic quantities of 64Cu using a 12 MeV cyclotron. *Nucl. Med. Biol.* **30**(5), 535–539 (2003).
23. Tanaka, T. et al. Double-tracer autoradiography with Cu-ATSM/FDG and immunohistochemical interpretation in four different mouse implanted tumor models. *Nucl. Med. Biol.* **33**(6), 743–750 (2006).
24. Okazawa, H. et al. Noninvasive method for measurement of cerebral blood flow using O-15 water PET/MRI with ASL correlation. *Eur. J. Radiol.* **105**, 102–109 (2018).
25. Okazawa, H. et al. Cerebral oxidative stress in early Alzheimer's Disease evaluated by 64Cu-ATSM PET/MRI: a preliminary study. *Antioxidants* **11**(5), 1022 (2022).
26. Dounousi, E. et al. Oxidative stress is progressively enhanced with advancing stages of CKD. *Am. J. Kidney Dis.* **48**(5), 752–760 (2006).
27. Nikolaev, A. V. et al. Pre-transplant kidney quality evaluation using photoacoustic imaging during normothermic machine perfusion. *Photoacoustics* **36**, 100596 (2024).
28. Atteia, H. H. et al. Soluble guanylate cyclase agonist, isoliquiritigenin attenuates renal damage and aortic calcification in a rat model of chronic kidney failure. *Life Sci.* **317**, 121460 (2023).
29. Stehle, D. et al. Novel soluble guanylyl cyclase activators increase glomerular cGMP, induce vasodilation and improve blood flow in the murine kidney. *Br. J. Pharmacol.* **179**(11), 2476–2489 (2022).
30. Ribeiro, M. et al. Sulforaphane upregulates the mRNA expression of NRF2 and NQO1 in non-dialysis patients with chronic kidney disease. *Free Radic Biol. Med.* **221**, 181–187 (2024).

Acknowledgements

Author contributions

HO and YH designed the study. YH, YN, MN, AM, TM and HO contributed to data acquisition. YH, YN and HO contributed to the data analysis and interpretation. HO calculated quantitative images. YH validated the quantitative values. YH and HO performed the statistical analysis. YH and HO contributed to drafting of the manuscript together. YN, MN, TM, AM, KY, TT and HO review and editing. All authors read and approved the final manuscript.

Declarations

Competing interests
The authors declare no competing interests.

Additional information
Correspondence and requests for materials should be addressed to H.O.

Reprints and permissions information is available at www.nature.com/reprints.

Publisher's note Springer Nature remains neutral with regard to jurisdictional claims in published maps and institutional affiliations.